A Data-Driven Method for Improving Historical Maps' Positional Accuracy

Konstantinos Vantas[1,*] and Vasiliki Mirkopoulou[2]

[1] Department of Rural and Surveying Engineering, Aristotle University of Thessaloniki, 54124 Thessaloniki, Greece

[2] Department of Informatics, Faculty of Science, University of Western Macedonia, 52100, Kastoria, Greece; vmirkopoulou@uowm.gr

* Correspondence: vantas@topo.auth.gr

Abstract: Positional accuracy improvement (PAI) of historical maps involves correcting their inherent geometric distortions, which often limit their usability in modern applications. Although resurveying an entire map provides the most accurate solution for PAI, it is costly, time-consuming, and often impossible. This study proposes a cost-effective, alternative data-driven method, using Generalized Additive Models (GAMs) to enhance positional accuracy, without requiring complete resurveying. GAMs were utilized within a statistical learning framework to: (a) identify spatial patterns of geometric errors; (b) systematically correct these errors; and (c) evaluate their generalization ability via spatial cross-validation. The method was tested on a 1925, urban cadastral, map from Greece, which was georeferenced and vectorized for the first time. A dataset of 2,287 homologous points from modern land surveying was compiled. To simulate sparce data conditions, 10% of these points were used for training and 90% for testing. The results revealed significant spatial structures in positional errors, and cross-validation confirmed the model's robustness. When applied to the test set, the fitted model doubled the spatial accuracy of the 1925 map, meeting the modern geometric standards set by the Greek National Cadastre. These findings

demonstrate the method's effectiveness and potential to enhance historical maps and other geospatial datasets that are facing similar issues across diverse research areas, such as urban planning and environmental history.

Keywords: positional accuracy improvement; Generalized Additive Models; historical cartography; data-driven methods; spatial cross validation; Greece.

1. Introduction

Accurate geospatial data are fundamental for a wide range of applications, from legal to urban planning and environmental modeling. Positional accuracy improvement (PAI) is a challenge arising from the need to refine the geometric attributes of a geospatial dataset, enhancing or homogenizing its absolute accuracy, given a specific reference system (Hashim et al. 2017). This need emerges in: (a) the creation of new spatial infrastructures, when integrating data of varying accuracies often leads to the problem of geometric conflation (Casado 2006); (b) existing spatial datasets generated by combining various sources using different technologies, surveying methods and accuracies (Sisman 2014); and (c) in spatial datasets derived from digitizing analogue maps that have non-uniform distortions (Tuno, Mulahusić, and Kogoj 2017). Over the past four decades, the demand for geospatial databases with progressively higher spatial accuracy has driven the development of processes and methods that aim to improve their geometric quality (Čeh et al. 2019; Felus 2007; Hope, Gordini, and Kealy 2008; Mjøs 2020; Tamim 1992; Vorel et al. 2010).

PAI is essential for historical maps that suffer from inherent inaccuracies. Researchers are using old topographic, cadastral, and military maps for applications in land use/cover change modeling, urban growth analysis, and in historical, societal, legal, and

environmental research (Leyk, Boesch, and Weibel 2005; Li et al. 2021; Piškinaitė and Veteikis 2023; Podobnikar 2010). Despite their usefulness, spatial datasets produced from digitizing historical maps display non-uniform and irregularly spatially distributed errors. These errors are caused by: (a) limitations of past surveying technologies; (b) faults introduced during hand-drawing cartography; (c) distortions from ageing and material degradation of physical maps; and (d) issues during the digitization and georeferencing phases into modern reference systems (Brovelli and Minghini 2012; Piškinaitė and Veteikis 2023; Tong, Shi, and Liu 2009; Tuno et al. 2017). Therefore, the positions of features on these datasets differ from their true ones due to both systematic and random errors. Such inaccuracies complicate the integration of old maps into modern geospatial databases.

Resurveying an entire spatial dataset is theoretically the optimal method to create one with higher accuracy. However, it is often unrealistic due to excessive costs and time constraints. Moreover, landscape changes in areas represented in historical maps can make complete resurveying impossible, both in urban and rural areas. Computational corrections offer a more feasible alternative. These methods transform existing datasets using a set of homologous points (corresponding features identified in both datasets) from higher-accuracy sources, such as global satellite navigation systems (Hope et al. 2008), photogrammetric diagrams (Ożóg 2020; Puniach et al. 2018), airborne LiDAR (Wierzbicki, Matuk, and Bielecka 2021), or conventional land surveys. Common techniques involve global transformations [e.g., Helmert (Watson 2006), affine (Morgenstern, Prell, and Riemer 1989)], surface-based transformations [e.g., rubber sheeting (Doytsher 2000), thin plate splines (Siriba, Dalyot, and Sester 2012; Tuno et al. 2017)], and geometric constraint-based approaches [e.g., triangulation (Čeh et al. 2019), areal limitations (Doytsher and Shmutter 1984)]. Hybrid methods that combine

these techniques have also been explored (Felus 2007; Tamim 1992; Zrinjski et al. 2019).

Most computational approaches for PAI of historical maps are deterministic and model-driven, relying on predefined mathematical equations, such as linear or polynomial functions. These methods assume uniform error patterns; however, historical maps often have heterogeneous distortions. Data-driven methods may be more effective for PAI of historical maps, where errors may lack uniformity, because they don't rely on predefined functions. Through learning algorithms, these methods can automatically identify both the spatial distribution of errors and their nonlinear relationships with covariates such as coordinates, terrain, and map edges. Nevertheless, applications using data-driven methods remain scarce. For instance, a recent study on the reconstruction of the Cadastral Map of the Netherlands (Franken et al. 2020) presents a combination of neural-networks and edge-matching algorithms in the digitization process of old maps.

In this study, we present a data-driven method based on Generalized Additive Models [GAMs (Hastie 1991)], a statistical learning algorithm, for PAI of historical maps. Examples of GAMs in spatial data analysis extend to various fields – epidemiology, ecology, remote sensing, and climate science – where they model COVID-19 mortality risk in Toronto (Feng 2022), predict species abundance in the Gulf of Mexico (Drexler and Ainsworth 2013), gap-fill Terra MODIS data (Guo et al. 2021), and interpolate spatial climate data (Bonsoms and Ninyerola 2024), respectively. Unlike many machine learning algorithms that often operate as black boxes [e.g. neural networks, random forests, (Handelman et al. 2019)], GAMs provide interpretability while remaining flexible enough to capture complex, non-linear relationships (Gareth et al. 2023). This balance between complexity and interpretability can improve the understanding of

geometric errors of old maps, distinguishing GAMs from less interpretable data-driven algorithms.

In our paper, we use a statistical learning framework aiming to: (a) identify spatial structures and anomalies in the geometric errors of old maps; (b) systematically correct these errors when they are not random; and (c) assess the model's generalization ability using a validation scheme. We demonstrate the efficiency of this method on one of the oldest urban cadastral maps of Greece, dated to 1925, highlighting its potential to meet modern geometric accuracy criteria. To our knowledge, this represents the first application of GAMs for PAI in historical cartography, offering both interpretability and adaptability to non-linear errors.

2. Materials and Methods

The methodology is summarized in Figure 1, which illustrates the workflow from input data (blue: digitized cadastral maps, land survey data) to intermediate datasets (orange), model outputs (green: fitted GAM, predicted test values), and, finally, results (grey: transformed cadastral maps, out-of-sample error of the test set).

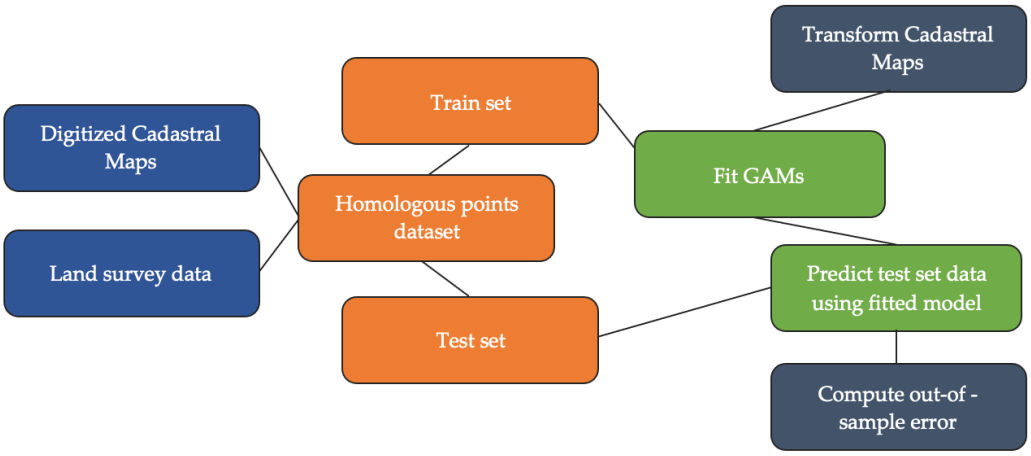

Figure 1. Flowchart of the applied methodology.

2.1. Study area and cadastral maps

The study area covers an area of 1 km^2 in Kastoria, a city in northwestern Greece (Figure 2) with a rich history and culture, particularly known for its Byzantine heritage and its unique urban morphology. The city contains numerous well-preserved architectural monuments constructed during different historical periods, including Byzantine, Ottoman, and early modern. These structures, and a significant portion of the city, are protected by both the Greek Ministry of Culture and the Greek Ministry of Environment and Energy. This underscores the need for accurate geospatial records to support heritage preservation and urban planning, ensuring that these elements are carefully integrated into the city's development plans.

Historically, the Greek National Cadastre faced numerous unsuccessful or incomplete attempts (Potsiou, Volakakis, and Doublidis 2001), until its current form initiated in 1995 and continues today. One of the earliest efforts was the cadastral survey study of Kastoria in 1925. This 1925 map has historical, sociological, and legal significance, documenting land ownership among diverse 20th-century communities (Christian, Jewish, Muslim) and depicting architectural monuments, some of which no longer exist (Tsolakis 1996).

Today 19 out of the 20 cadastral diagrams (in a scale 1:500), along with the alphabetical index of apparent owners, are preserved in the archives of the Urban Development Department of Kastoria Municipality. Unfortunately, no raw measurements from land surveying, nor details of the triangulation processes or traverse networks, are available for these diagrams. Parcels from the missing map were reconstructed using archived old topographic maps from the same Department to create a complete dataset for analysis.

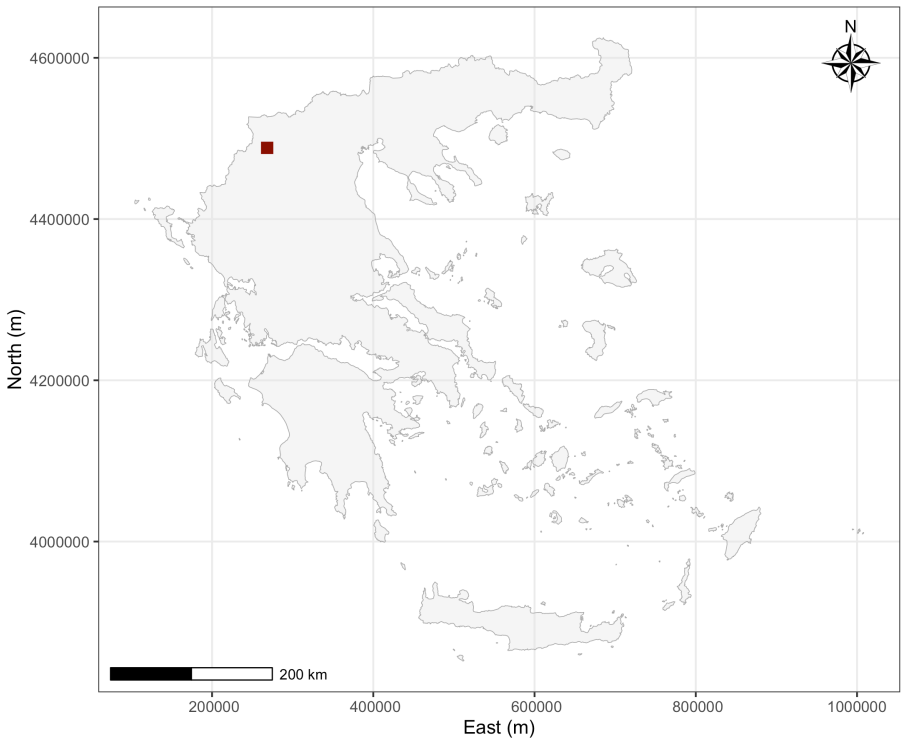
N
4600000
4400000
4200000
4000000
North (m)
200 km
200000
400000
600000
800000
1000000
East (m)

(a)

(b)

Figure 2. (a) The study area location in Greece (dark red box). Reference System: HGRS87 (Hellenic Geodetic Reference System, 1987); (b) Orthophoto map of the study area (2015), source: National Cadastre of Greece.

2.2 Digitization and homologous points

The 1925 cadastral diagrams were scanned and georeferenced using rubber-sheeting with the QGIS software (QGIS Development Team 2025). Subsequently, the entire set of 1,392 parcels and 2,204 buildings was digitized into vector format (shapefiles) and transformed from the old Greek Datum [GR-Datum, (Fotiou and Livieratos 2000)] to the Hellenic Geodetic Reference System 1987 [HGRS87, (Veis 1995)], the official coordinate system for surveying applications in Greece, using the second degree polynomials method as given by Hellenic Mapping and Cadastral Organization (Hellenic Mapping and Cadastral Organization 1995). The produced geospatial database is depicted in Figure 3.

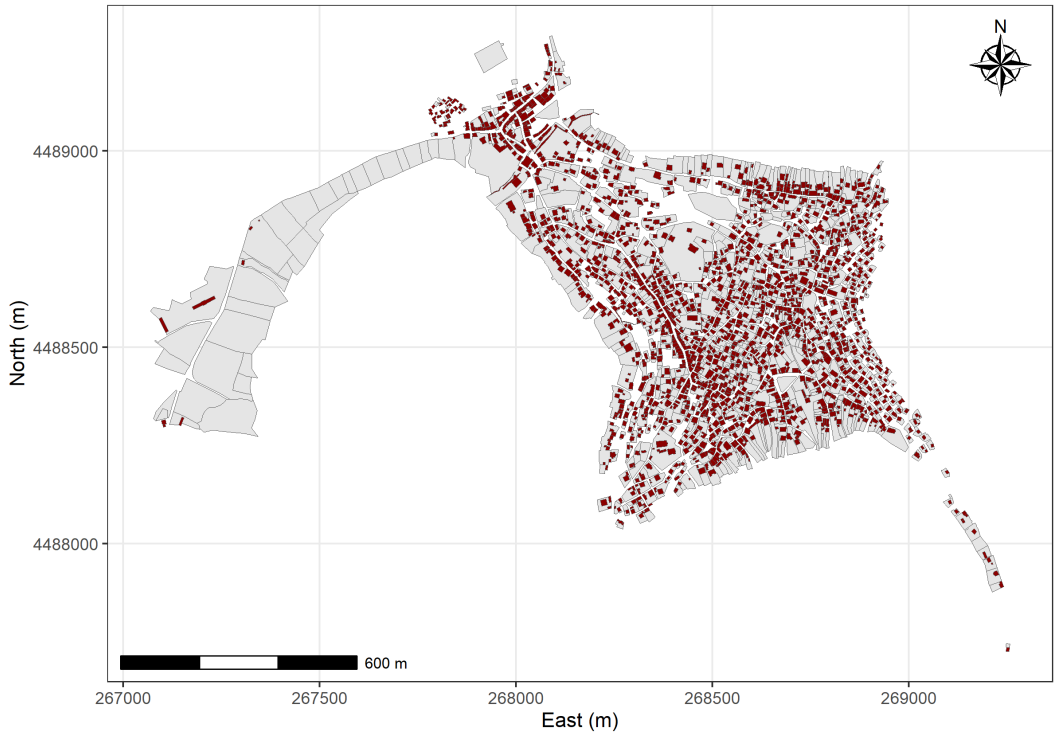

Figure 3. Digitized parcels and buildings from Kastoria's 1925 Cadastral map. Parcels are depicted in grey and buildings in red.

To determine positional errors, homologous points were identified by comparing coordinates of building corners between the 1925 map and a more accurate, digital topographic study performed by the Municipality of Kastoria in 1996, which employed modern surveying instruments and techniques. This 1996 study was based on land surveying at a scale of 1:500 and is considered the most accurate, available, geospatial data for the area of interest.

Coordinate differences were calculated as:

$$DE_i = E0_i - E1_i$$
$$DN_i = N0_i - N1_i \quad (1)$$

where the Easting/Northing differences DE_i and DN_i are the differences along the x-axis and the y-axis, respectively, for point i. In this form, the vector $[E0_i, N0_i]$

represents the coordinates from the 1925 map and $[E1_i, N1_i]$ from the 1996 land survey. As a result, a dataset of 2,287 homologous points was generated.

2.3 Generalized Additive Models

GAMs extend Generalized Linear Models (GLMs) by fitting a set of smoothing functions for each input (predictor) variable and then summing these contributions to estimate an output (response)(Hastie and Tibshirani 1986). This extension allows GAMs to capture complex non-linear relationships between the inputs and the output, which is essential for modelling the spatially variable distortions in historical maps.

In contrast to traditional linear regression or standard GLMs, GAMs can produce more accurate results when non-linear relationships are present (Hastie, Friedman, and Tibshirani 2001). Moreover, they are, generally, more interpretable than other machine learning methods, as already noted, since the individual effects of each predictor can be visualized and analyzed (Gareth et al. 2023).

A GAM takes the form of smooth functions of each predictor (Hastie and Tibshirani 1986):

$$g(\mathbb{E}(y|\boldsymbol{X}) = \alpha + \sum_{j=1}^{m} s_j(x_j) \quad (2)$$

where g is a link function (e.g. the identity or log functions), α is the intercept (bias), s_j is a smooth function of the j^{th} input variable x_j and y the output.

The smooth functions $s_j(x)$are typically constructed using a set of basis functions:

$$s(x) = \sum_{i=1}^{n} b_i(x) \cdot \beta_i \quad (3)$$

where $b_i(x)$ is the basis function with index i and β_i are the unknown coefficients.

As showed in Equation 3, each smooth function, each smooth function $s(x)$ is itself represented as a linear combination of basis functions $b_i(x)$, with coefficients β_i, that the model learns from the data.

Common choices for basis functions include polynomial functions and splines. Efficient computational procedures exist for selecting the optimal form and degree of smoothness for the basis functions. In practice, these procedures are implemented in software packages such as the R language (R Core Team 2025) packages *gam* (Hastie 2024) and *mgcv* (Wood 2017), which typically use criteria like generalized cross-validation (GCV), or restricted maximum likelihood (REML), to control the smoothness and prevent overfitting. For further details on alternative fitting methods and applications, see Breiman and Friedman (Breiman and Friedman 1985), Hastie and Tibshirani (Hastie and Tibshirani 1987), Wood (Wood 2010), and Wood et al. (Wood, Pya, and Säfken 2016).

For this study, a bivariate GAM modelled DE and DN as:

$$\begin{aligned} DE &= a_1 + s_1(E0, N0) + \varepsilon_{DE} \\ DN &= a_2 + s_2(E0, N0) + \varepsilon_{DN} \end{aligned} \tag{4}$$

where $E0$ and $N0$ are the coordinates of the old map, and the error residuals ε_{DE} and ε_{DN} are assumed to be bivariate normal:

$$\begin{bmatrix} \varepsilon_{DE} \\ \varepsilon_{DN} \end{bmatrix} \sim \mathcal{N}\left(\begin{bmatrix} 0 \\ 0 \end{bmatrix}, \begin{bmatrix} \sigma_{DE}^2 & \sigma_{DE,DN} \\ \sigma_{DE,DN} & \sigma_{DN}^2 \end{bmatrix} \right) \tag{5}$$

where a_1 and a_2 are the intercepts for the DE and DN equations respectively; s_1 and s_2 are two-dimensional smooth functions, estimated non-parametrically using penalized thin plate regression splines (Wood 2003); σ_{DE}^2 and σ_{DN}^2 are the variances; and $\sigma_{DE,DN}$

the covariance. Smoothing parameters were optimized using REML with the R package *mgcv* (Wood 2017). The bivariate normal assumption (Equation 5) for the error residuals was selected in order to represent spatially correlated errors, allowing a dependence among them.

In practical terms, for a given point on the old map, the model predicts the systematic shift in easting and northing, reflecting how the 1925 map coordinates deviate from the higher precision land survey. By these non-linear functions the GAM provides a flexible representation of systematic errors of the old map.

An advantage of using GAMs with penalized thin plate splines is their behavior in extrapolation. More specifically, with the default second-derivative penalty, these splines act as linear functions in areas with no training data. This controlled behavior ensures predictable transformations of the 1925 map, avoiding the creation of erratic artifacts often produced by other non-linear machine learning algorithms, such as neural networks (Xu et al. 2021; Zhu et al. 2023).

2.4 Validation scheme and error metric

The dataset was randomly split into a 10% training and a 90% testing set (Figure 4a). This unusual ratio simulates real-world scenarios of historical maps where homologous points are sparse due to landscape changes over time or limited availability. When evaluating learning algorithm performance, data are often assumed to be independent (Gareth et al. 2023). However, in geospatial datasets, point data tend to be more strongly correlated when they are closer together (Cressie 1993). This phenomenon of spatial autocorrelation implies that using a classical cross-validation method can lead to biased—and overly optimistic—error estimates (Valavi et al. 2019).

To address spatial autocorrelation, this study uses a spatial cross validation (SCV) method on the training set (Pohjankukka et al. 2017). In this approach, the sampling of data points for error estimation is based on their spatial structure (e.g. a data split is created for contiguous groups of points). Particularly, the k-means algorithm (Hartigan and Wong 1979:136), as implemented in the R language (R Core Team 2025), is chosen to partition the dataset for its effectiveness, with the coordinates of the points serving as input variables. The number of clusters is set to ten (Figure 4b), a value that is empirically used in cross-validation schemes (Kuhn and Johnson 2013).

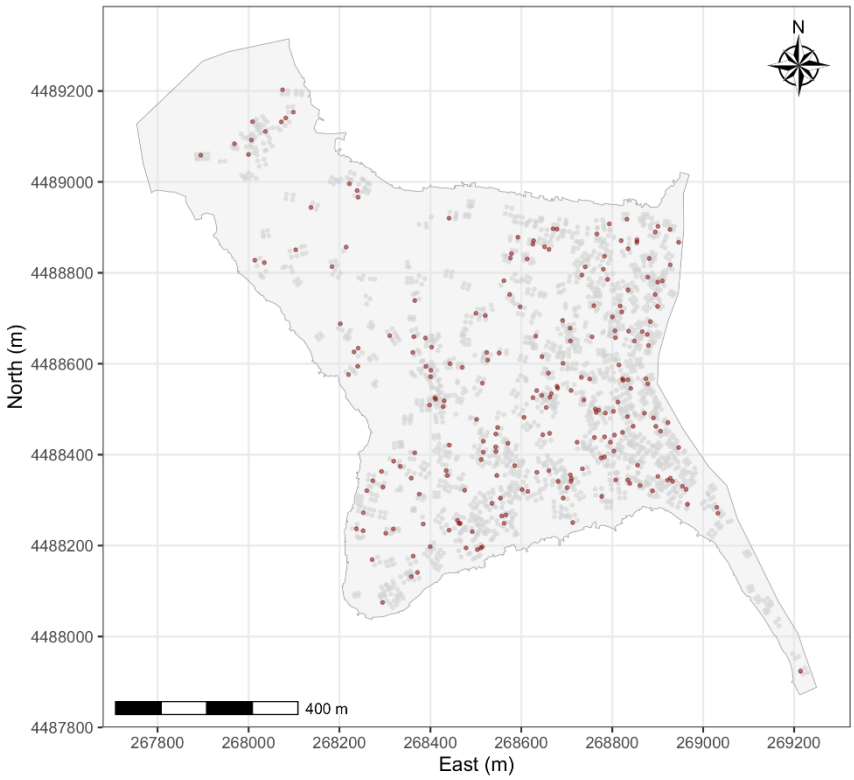

(a)

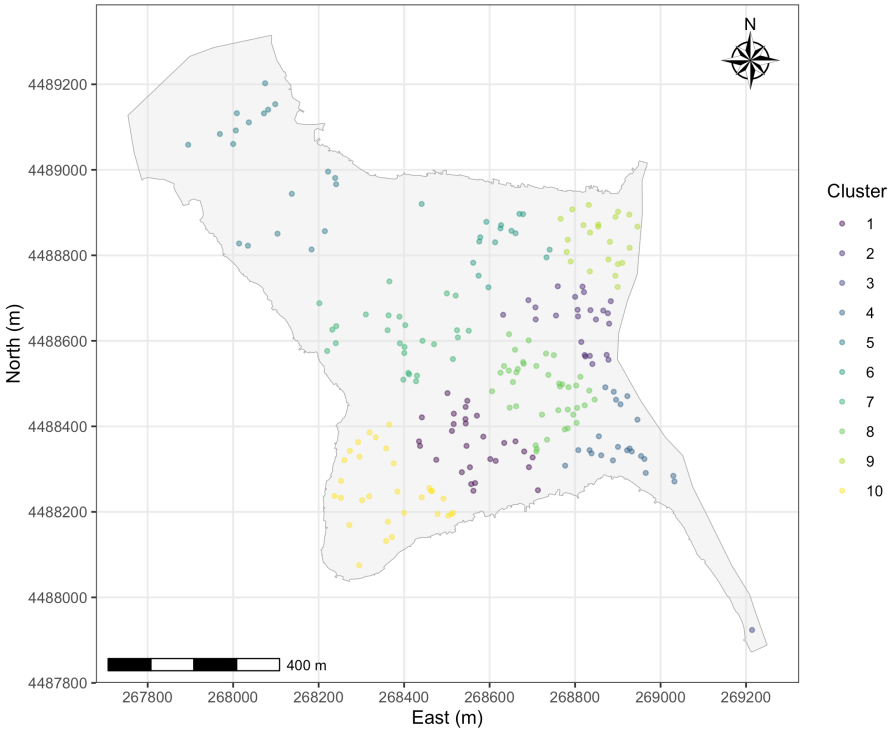

(b)

Figure 4. (a) Red points indicate the homologous points randomly selected for the training set, while grey points represent those in the testing set; (b) different colors denote the clusters of training sets used in the cross-validation scheme.

Model performance was evaluated using the root mean squared error (RMSE) in Euclidean space:

$$RMSE_{E,N} = \sqrt{\frac{1}{n}\sum_{i=1}^{n}\left(\left(E1_i - \widehat{E1}_i\right)^2 + \left(N1_i - \widehat{N1}_i\right)^2\right)}$$

$$RMSE_E = \sqrt{\frac{1}{n}\sum_{i=1}^{n}\left(\left(E1_i - \widehat{E1}_i\right)^2\right)} \quad (6)$$

$$RMSE_N = \sqrt{\frac{1}{n}\sum_{i=1}^{n}\left(\left(N1_i - \widehat{N1}_i\right)^2\right)}$$

Where $RMSE_{E,N}$ is the 2D RMSE, while $RMSE_E$ and $RMSE_N$ are 1D RMSE in Easting and Northing respectively, $[\widehat{E1}_i, \widehat{N1}_i]$ are the corrected coordinates of the 1925 map from the fitted GAM predictions $\widehat{DE}_i$ and $\widehat{DN}_i$, with: $\widehat{E1}_i = E0_i - \widehat{DE}_i$ and $\widehat{N1}_i = N0_i - \widehat{DN}_i$.

It is important to note that the homologous points' coordinates $E1_{\mathrm{i}}$, $N1_{\mathrm{i}}$ from the 1996 land survey also have inherent variance due to the uncertainty of these measures. This variance can be theoretically estimated using error propagation combining factors such as the initial control point variance, network geometry, and equipment accuracy (Fotiou and Livieratos 2000) (e.g., triangulation, traverses, and angular and distance measurements). However, in PAI studies the coordinates of higher precision are considered to have perfect accuracy, which may lead to an underestimation of the total, true, positional uncertainty of the model.

The RMSE error metrics of Equation 6 are the same type of metrics used in the modern geometric accuracy criteria of the Greek National Cadastre, where positional accuracy is evaluated based on errors in mapping of well-defined ground points that appear on the orthophoto maps, and verification is conducted through random sampling and land surveying to ensure compliance with the technical specifications (Hellenic Republic 2016).

3. Results and Discussion

3.1 Exploratory analysis

The positional differences (DE and DN) between the 1925 map and the 1996 survey, and their Euclidean distances L were analyzed using central moments (mean, standard deviation, skewness and kurtosis), the median and coefficient of variation (Table 1). The key observations about these values are:

- Skewness: Near-zero values suggest approximately symmetric distributions;
- Kurtosis: Low values indicate light tails, consistent with normal-like distributions;
- Variability: The Coefficient of Variation (CV) is higher for DE and DN individually, indicating more relative variability in Easting and Northing errors separately, compared to the overall positional error magnitude (L).

Table 1. The average statistical properties of the differences DE and DN and the corresponding Euclidean distances L of homologous points. SD is an abbreviation for standard deviation and CV for coefficient of variation (SD/Mean). All values except skew, kurtosis and CV are in meters.

Metric	Min	Mean	Median	Max	SD	Skew	Kurtosis	CV
DE	-1.29	0.52	0.55	2.46	0.46	-0.17	0.19	0.83
DN	-1.74	-0.20	-0.22	1.61	0.47	0.29	0.43	2.10
L	0.00	0.77	0.77	2.49	0.37	0.38	0.19	0.48

Figure 5 illustrates the spatial structure of L using vectors as oriented arrows. In this plot, each arrow's length corresponds to the magnitude of L, while its direction indicates

the angle of the difference. This representation shows that the differences DE and DN are not randomly distributed but, instead, follow a spatial pattern. Lower values of L are observed in the southwest, and, generally, a clockwise-like rotation exists in the remaining area of the study, suggesting a consistent angular distortion across much of the map. This structure justifies the modeling of systematic errors rather to attribute them to random noise.

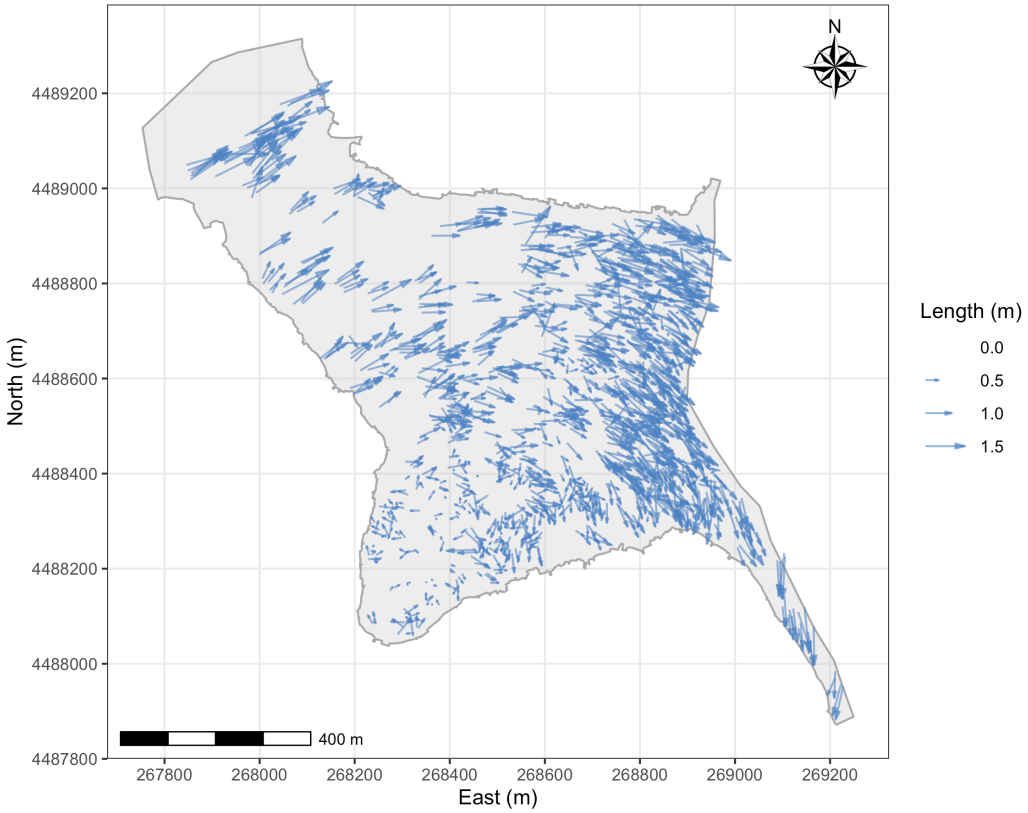

Figure 5. Oriented arrows represent the Euclidean distances between homologous points: each arrow's length corresponds to the value in meters, while its direction indicates the orientation of the difference.

3.2 Model performance and interpretation

The GAM was evaluated versus a baseline identity model (i.e. $\widehat{E1}_i = E0_i$ and $\widehat{N1}_i = N0_i$), which assumes no positional correction. This comparison highlights the GAM's ability to systematically address the spatially structured errors that exist in the 1925

cadastral map. Table 2 summarizes the RMSE for both models for the SCV, training and testing datasets.

Table 2. Error metrics of the GAM and an identity model for comparison. SCV is an abbreviation for spatial cross validation. Error metric values in red indicate those that do not meet the modern geometric accuracy criteria of the Hellenic Cadastre. All values are in meters.

Metric	**Baseline**			**GAM**		
	SCV	**Train**	**Test**	**SCV**	**Train**	**Test**
$RMSE_{E,N}$	0.91	0.88	0.85	0.36	0.39	0.44
$RMSE_{E}$	0.66	0.72	0.68	0.25	0.28	0.32
$RMSE_{N}$	0.56	0.51	0.51	0.25	0.28	0.30

The baseline model's error metrics are identical with the positional inaccuracies of the 1925 cadastral map. These metrics surpass the modern Greek National Cadastre's geometric accuracy criteria: $RMSE_{(E,N)} \leq 0.56$, $RMSE_{(E)} \leq 0.40$ and $RMSE_{(N)} \leq 0.40$ in meters. On the other hand, the application of the GAM reduced errors by approximately 50%, accomplishing error metrics that align with the present-day standards in Greece.

The matching values of RMSE among the training, cross-validation, and testing set imply that the trained model does not overfit data, providing strong evidence about its generalization ability to new, unseen, data. Otherwise, the model would not only capture the spatial patterns of errors, but also random noise.

For context, similar studies applying different correction methods have reported varying levels of PAI. Polynomial fitting of Como's historical cadastral maps achieved RMSE in the range of 3–10 m (Brovelli and Minghini 2012). In Slovenia the membrane adjustment method improved the accuracy of, also cadastral maps, to approximately 1 m (Čeh et al. 2019). In Victoria, Australia a hybrid method applied to historical maps resulted accuracies between 3 and 5 m (Hope et al. 2008). (d) in Turkey, affine transformation on a modern 1990 cadastral map reduced positional variance to approximately 0.20 m (Sisman 2014). Compared to these studies, our model demonstrated very satisfactory results, especially considering the differences in datasets, methodologies, and background across them.

Table 3 reports the summary output of the model fitted on the training data. Various values are reported, including the estimated degrees of freedom (EDF) for each smooth term, along with the corresponding test statistics (e.g., z-values and chi-square values) regarding the statistical significance of GAMs' terms and their p-values.

Table 3. Summarized results from the GAM model fitted on the training data. Estimated degrees of freedom (EDF) identifies the non-linearity of the smooth terms. Reference degrees of freedom (RDF) are used to compute chi-square. Z-values and chi-square values are used to compute the approximate p-values of the terms.

Response	**Component**	**Term**	**Estimate**	**Standard Error**	**z-value**	**p-value**
DE	A. Parametric coefficients	a_1	0.53	0.02	29.16	$< 2 \cdot 10^{-16}$
DN		a_2	-0.22	0.02	-11.86	$< 2 \cdot 10^{-16}$
Response	**Component**	**Term**	**EDF**	**RDF**	**Chi-square**	**p-value**
DE	B. Smooth terms	$s_1(E0, N0)$	17.99	22.83	447	$< 2 \cdot 10^{-16}$
DN		$s_2(E0, N0)$	8.77	12.16	375	$< 2 \cdot 10^{-16}$

Both the intercepts a_1 and a_2 of the linear component are statistically significant, as are the smooth terms $s_1(E0, N0)$ and $s_2(E0, N0)$, indicating that all terms make meaningfully contributions to explain the systematic errors of the 1925 map ($p < 2 \cdot 10^{-16}$). The intercepts $a_1 = 0.53$ m and $a_2 = -0.22$ m represent global offsets in DE and DN likely due to systematic errors in the triangulation survey process of the old map.

The nonlinear spatial patterns captured by $s_1(E0, N0)$ and $s_2(E0, N0)$ regard more localized errors. The higher EDF of s_1 (Figure 6a) compared to s_2 (Figure 6b) suggests a more complex, non-linear spatial pattern for DE, potentially related to historical surveying and mapping practices and the form of the traverse networks.

The model explains 65% of the deviance, with the estimated standard deviations of $\sigma_{DE} = 0.27$ m, $\sigma_{DN} = 0.28$ m, and a covariance $\sigma_{DE,DN} = 0.002$ m^2. This means that the GAM captures approximately two-thirds of the systematic variability in the output variables compared to a perfect model, a robust result for real-world spatial data, leaving the remaining one-third to be random noise or unmodeled factors.

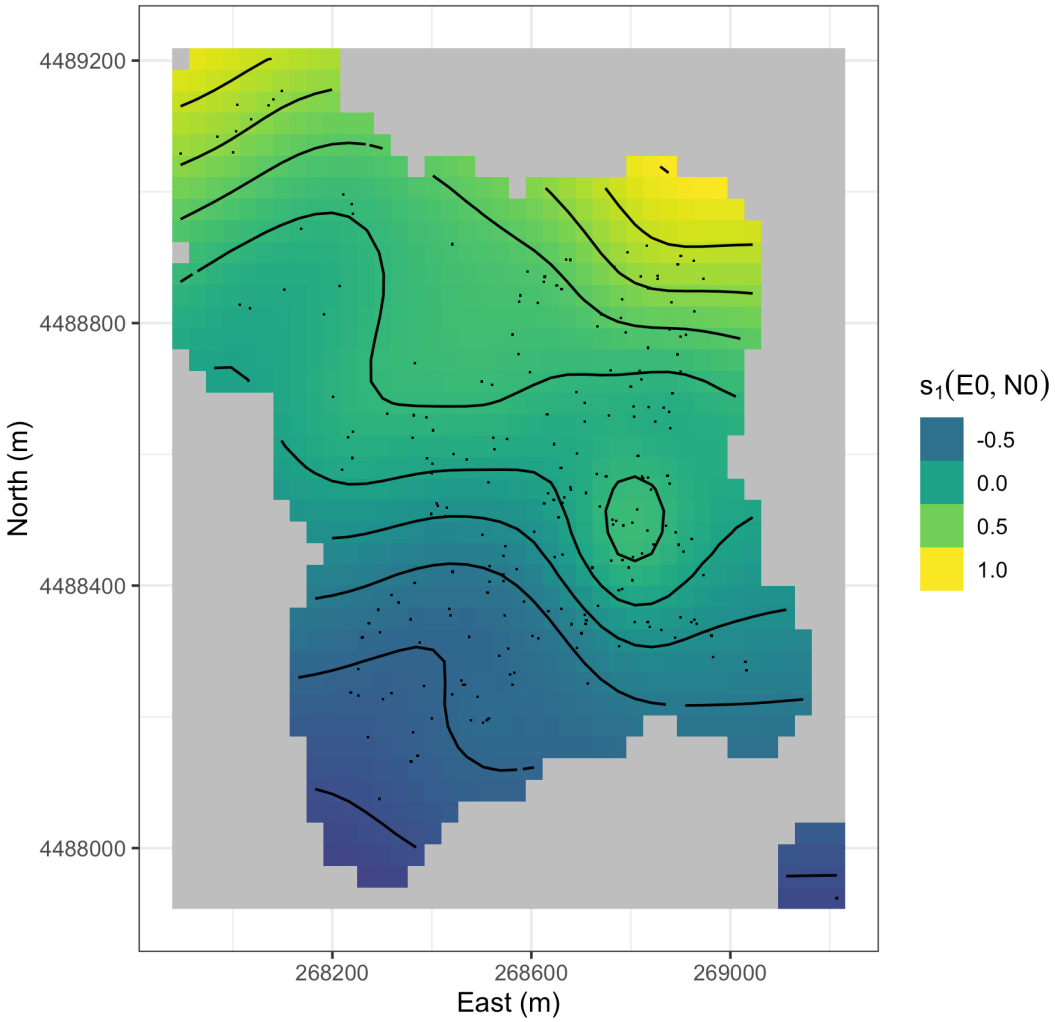
4489200
4488800
4488400
4488000
North (m)
268200
268600
269000
East (m)
s_1(E0, N0)
-0.5
0.0
0.5
1.0

(a)

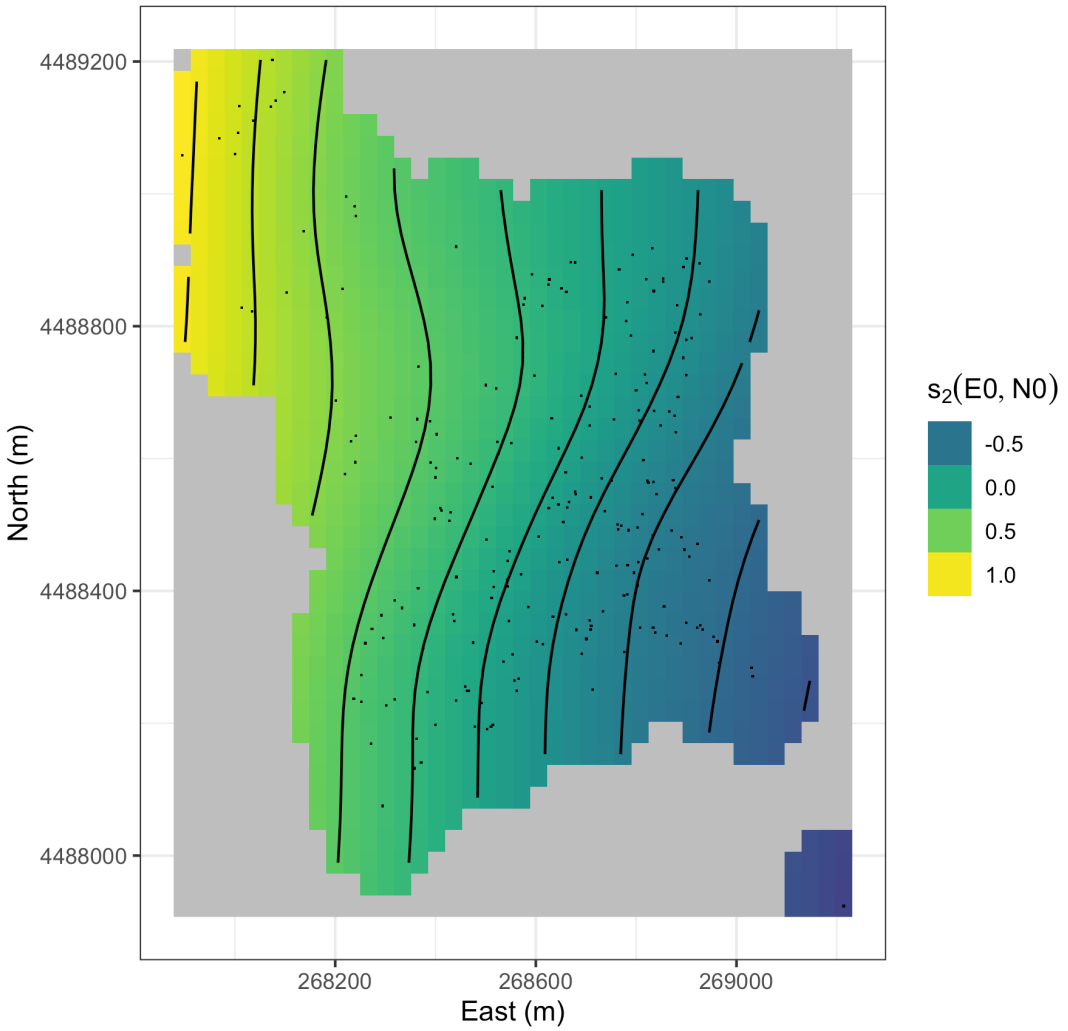

(b)

Figure 6. (a) Partial effect plot of smooth term $s_1(E0, N0)$; (b) Partial effect plot of smooth term $s_2(E0, N0)$. All values are in meters. With black dots are the points of the training data set and with black lines the isopleths of partial effects values.

The correlation between residuals ε_{DE} and ε_{DN} calculated as $\rho = \sigma_{DE,DN}/(\sigma_{DE} \cdot \sigma_{DN}) = 0.02$, implies that very little to no linear relationship exist between them. While this negligible shared variance suggests near-independence between the residuals, it does not invalidate the selection of a bivariate GAM. On the contrary, it means that there are no other unobserved input variables that affect both DE

and DN similarly. Specifically, the bivariate model considers potential covariance between output responses that could not be known in advance, offering a more robust evaluation of prediction uncertainty than two separate univariate GAMs.

Residual errors ε_{DE} and ε_{DN} are depicted as vectors (directional arrows) in Figure 7, revealing no visible spatial structures, in contrast to the systematic patterns in the 1925 map (Figure 5). This absence of autocorrelation verifies that the GAM successfully captured systematic errors, leaving error residuals that represent the random noise of the old map.

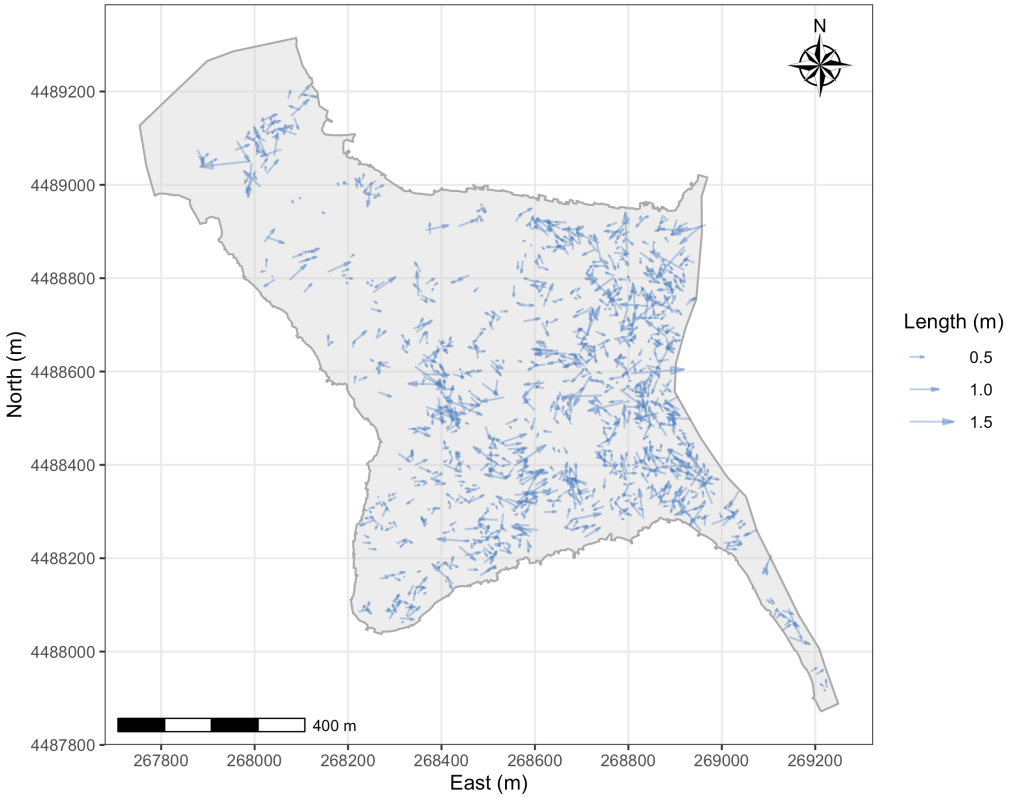

Figure 7. Oriented arrows represent the residuals of the model: each arrow's length corresponds to the value in meters, while its direction indicates the orientation of the residual.

Figure 8 presents the transformed 1925 cadastral map using the trained GAM (a portion of the map). Several common buildings and parcel boundaries can be identified on the orthophoto background, demonstrating the accuracy of the proposed method.

Figure 8. Transformation of the 1925 cadastral map into vector format using the trained GAM. Buildings from the old map are outlined in blue, while land parcels are shown in black. The numbers inside the buildings indicate the number of floors, and the parcel codes correspond to the six-digit numbers (both from the 1925 map). The background is an orthophoto map of the area from the Greek National Cadastre (2015).

4. Conclusions

This study makes a significant contribution to the field of historical cartography by introducing a novel and effective data-driven method, utilizing Generalized Additive Models (GAMs) to substantially improve the positional accuracy of historical maps. The method was tested on one of the oldest urban cadastral maps in Greece (1925) which was georeferenced and vectorized into a spatial database for the first time. The model reduced the errors of the 1925 map by approximately 50%, achieving accuracy metrics that align with the present-day standards of the National Cadastre of Greece.

GAMs successfully recognized non-uniform and irregularly spatially distributed errors, leveraging their inherent interpretability and ability to model complex non-linear spatial relationships, as designed. Spatial cross-validation and a testing dataset that simulates real-world scenarios where homologous points are sparse, confirmed the model's ability to perform equally well on new and unseen data, with consistent RMSE values of 0.39 m (training), 0.36 m (cross-validation), and 0.44 m (testing). The corrected 1925 map can be seamlessly integrated into modern geospatial databases, demonstrating its considerable practical utility, supporting urban planning, legal disputes, and heritage preservation in Kastoria, a city with significant Byzantine, Ottoman, and Early Modern monuments.

Beyond the city of Kastoria, the proposed method can assist researchers in the integration process of historical topographic, cadastral, and military maps for applications in land use/cover change modeling, urban growth analysis, and in historical, societal, legal, and environmental research. However, the method's dependence on homologous points does present limitations. Its applicability might be reduced in rural or heavily altered urban areas where homologous points are scarce or do not represent adequately the spatial distribution of errors. Additionally, the method requires the presence of systematic errors in the historical maps and not only random noise.

Future research could develop hybrid models that combine GAMs with deep neural networks. In these hybrid models the processes of digitizing and identification of homologous points or edge detection could be automated, using the pattern recognition capabilities of neural networks in conjunction with GAMs' interpretability and flexibility in spatial error modeling. Also, applying this method to various historical maps would further assess its broader applicability. To summarize, data-driven methods

can provide flexible, interpretable, and robust means to improve positional accuracy of geospatial datasets with similar issues. Future research in this domain could further extend their impact across broader research areas.

Acknowledgments: The authors would like to express their gratitude to the Urban Development Department of Kastoria Municipality, for providing access to the cadastral diagrams of 1925 and digital survey data of the city, which made this research possible.

Abbreviations

The following abbreviations are used in this manuscript:

GAM	Generalized Additive Model
PAI	Positional Accuracy Improvement
COVID-19	Coronavirus Disease 2019
CV	Coefficient of Variation
EDF	Effective Degrees of Freedom
GLM	Generalized Linear Model
HGRS87	Hellenic Geodetic Reference System 1987
LiDAR	Light Detection and Ranging
MODIS	Moderate Resolution Imaging Spectroradiometer
QGIS	Quantum Geographic Information System
RMSE	Root Mean Square Error
SCV	Spatial Cross Validation
SD	Standard Deviation
GCV	Generalized Cross-Validation
REML	Restricted Maximum Likelihood
RDF	Reference Degrees of Freedom

References

Bonsoms, Josep, and Miquel Ninyerola. 2024. “Comparison of Linear, Generalized Additive Models and Machine Learning Algorithms for Spatial Climate Interpolation.” *Theoretical and Applied Climatology* 155(3):1777–92. doi: 10.1007/s00704-023-04725-5.

Breiman, Leo, and Jerome H. Friedman. 1985. “Estimating Optimal Transformations for Multiple Regression and Correlation.” *Journal of the American Statistical Association* 80(391):580–98. doi: 10.1080/01621459.1985.10478157.

Brovelli, Maria A., and Marco Minghini. 2012. “Georeferencing Old Maps: A Polynomial-Based Approach for Como Historical Cadastres.” *E-Perimetron* 7(3):97–110.

Casado, Mara Luisa. 2006. “Some Basic Mathematical Constraints for the Geometric Conflation Problem.” Pp. 264–74 in *Proceedings of the 7th international symposium on spatial accuracy assessment in natural resources and environmental sciences*. Lisbon, Portugal.

Čeh, Marjan, Frank Gielsdorf, Barbara Trobec, Mateja Krivic, and Anka Lisec. 2019. “Improving the Positional Accuracy of Traditional Cadastral Index Maps with Membrane Adjustment in Slovenia.” *ISPRS International Journal of Geo-Information* 8(8):338. doi: 10.3390/ijgi8080338.

Cressie, Noel. 1993. *Statistics for Spatial Data*. Revised Edition. New York, USA: John Wiley & Sons.

Doytsher, Y., and B. Shmutter. 1984. “Adjustment of Information Digitized from Maps.” *Survey Review* 27(211):211–20. doi: 10.1179/sre.1984.27.211.211.

Doytsher, Yerahmiel. 2000. “A Rubber Sheeting Algorithm for Non-Rectangular Maps.” *Computers & Geosciences* 26(9–10):1001–10. doi: 10.1016/S0098-3004(00)00023-6.

Drexler, Michael, and Cameron H. Ainsworth. 2013. “Generalized Additive Models Used to Predict Species Abundance in the Gulf of Mexico: An Ecosystem Modeling Tool” edited by A. Davies. *PLoS ONE* 8(5):e64458. doi: 10.1371/journal.pone.0064458.

Felus, Yaron A. 2007. “On the Positional Enhancement of Digital Cadastral Maps.” *Survey Review* 39(306):268–81. doi: doi.org/10.1179/175227007X197183.

Feng, Cindy. 2022. “Spatial-Temporal Generalized Additive Model for Modeling COVID-19 Mortality Risk in Toronto, Canada.” *Spatial Statistics* 49:100526. doi: 10.1016/j.spasta.2021.100526.

Fotiou, A., and E. Livieratos. 2000. *Geometric geodesy and networks*. Thessaloniki, Greece: Editions Ziti.

Franken, Jeroen, Wim Florijn, Maarten Hoekstra, and Eric Hagemans. 2020. "Rebuilding the Cadastral Map of The Netherlands, the Artificial Intelligence Solution." in *FIG working week*. Amsterdam, the Netherlands.

Gareth, James, Daniela Witten, Trevor Hastie, and Robert Tibshirani. 2023. *An Introduction to Statistical Learning with Applications in R*. Second Edition. Switzerland: Springer.

Guo, Dianfan, Cuizhen Wang, Shuying Zang, Jinxi Hua, Zhenghan Lv, and Yue Lin. 2021. "Gap-Filling of 8-Day Terra MODIS Daytime Land Surface Temperature in High-Latitude Cold Region with Generalized Additive Models (GAM)." *Remote Sensing* 13(18):3667. doi: 10.3390/rs13183667.

Handelman, Guy S., Hong Kuan Kok, Ronil V. Chandra, Amir H. Razavi, Shiwei Huang, Mark Brooks, Michael J. Lee, and Hamed Asadi. 2019. "Peering Into the Black Box of Artificial Intelligence: Evaluation Metrics of Machine Learning Methods." *American Journal of Roentgenology* 212(1):38–43. doi: 10.2214/AJR.18.20224.

Hartigan, John A., and Manchek A. Wong. 1979. "Algorithm AS 136: A k-Means Clustering Algorithm." *Journal of the Royal Statistical Society. Series c (Applied Statistics)* 28(1):100–108. doi: 10.2307/2346830.

Hashim, N. M., A. H. Omar, S. N. M. Ramli, K. M. Omar, and N. Din. 2017. "Cadastral Database Positional Accuracy Improvement." *The International Archives of the Photogrammetry, Remote Sensing and Spatial Information Sciences* 42:91–96. doi: isprs-archives-XLII-4-W5-91-2017.

Hastie, Trevor. 2024. "Gam: Generalized Additive Models." Retrieved February 25, 2025 (https://CRAN.R-project.org/package=gam).

Hastie, Trevor, Jerome Friedman, and Robert Tibshirani. 2001. *The Elements of Statistical Learning*. Second Edition. New York, USA: Springer New York.

Hastie, Trevor J. 1991. "Generalized Additive Models." Pp. 249–307 in *Statistical models in S*. United Kingdom: Chapman & Hall.

Hastie, Trevor, and Robert Tibshirani. 1986. "Generalized Additive Models." *Statistical Science* 1(3):297–310. doi: 10.1214/ss/1177013604.

Hastie, Trevor, and Robert Tibshirani. 1987. "Generalized Additive Models: Some Applications." *Journal of the American Statistical Association* 82(398):371–86. doi: 10.1080/01621459.1987.10478440.

Hellenic Mapping and Cadastral Organization. 1995. *Tables of coefficients for coordinates transformation of the Hellenic area*. *Technical specifications*. Athens, Greece: HEMCO.

Hellenic Republic. 2016. *Approval of technical specifications and the regulation of estimated fees for cadastral survey studies for the creation of the National Cadastre in the remaining areas of the country*. *Technical specifications*. 15649. Athens, Greece: Ministry of Environment and Energy.

Hope, S., C. Gordini, and A. Kealy. 2008. “Positional Accuracy Improvement: Lessons Learned from Regional Victoria, Australia.” *Survey Review* 40(307):29–42. doi: doi.org/10.1179/003962608X253457.

Kuhn, Max, and Kjell Johnson. 2013. *Applied Predictive Modeling*. New York, USA: Springer New York.

Leyk, Stefan, Ruedi Boesch, and Robert Weibel. 2005. “A Conceptual Framework for Uncertainty Investigation in Map-Based Land Cover Change Modelling.” *Transactions in GIS* 9(3):291–322. doi: 10.1111/j.1467-9671.2005.00220.x.

Li, Shuang, Zhongqiu Sun, Yafei Wang, and Yuxia Wang. 2021. “Understanding Urban Growth in Beijing-Tianjin-Hebei Region over the Past 100 Years Using Old Maps and Landsat Data.” *Remote Sensing* 13(16):3264.

Mjøs, Leiv Bjarte. 2020. “Cadastral Development in Norway: The Need for Improvement.” *Survey Review* 52(375):473–84. doi: 10.1080/00396265.2019.1637094.

Morgenstern, D., K. M. Prell, and H. G. Riemer. 1989. “Digitisation and Geometrical Improvement of Inhomogeneous Cadastral Maps.” *Survey Review* 30(234):149–59. doi: 10.1179/sre.1989.30.234.149.

Ożóg, Karol. 2020. “The Use of Unmanned Aerial Vehicles for the Assessment of Land Boundaries Accuracy.” *Journal of Water and Land Development* (45). doi: 10.24425/jwld.2020.133050.

Piškinaitė, Eglė, and Darijus Veteikis. 2023. “The Results of Digitizing Historical Maps: Comparison of Lithuanian Land-Use Structure in the 19th and 21st Centuries.” *Land* 12(5):946. doi: 10.3390/land12050946.

Podobnikar, T. 2010. “Historical Maps of Ljubljana for GIS Applications.” doi: 10.1556/ageod.45.2010.1.12.

Pohjankukka, Jonne, Tapio Pahikkala, Paavo Nevalainen, and Jukka Heikkonen. 2017. “Estimating the Prediction Performance of Spatial Models via Spatial K-Fold Cross Validation.” *International Journal of Geographical Information Science* 31(10):2001–19. doi: 10.1080/13658816.2017.1346255.

Potsiou, Chryssy, Manolis Volakakis, and Periklis Doublidis. 2001. “Hellenic Cadastre: State of the Art Experience, Proposals and Future Strategies.” *Computers, Environment and Urban Systems* 25(4–5):445–76. doi: 10.1016/S0198-9715(00)00048-X.

Puniach, Edyta, Agnieszka Bieda, Paweł Ćwiąkała, Anita Kwartnik-Pruc, and Piotr Parzych. 2018. “Use of Unmanned Aerial Vehicles (UAVs) for Updating Farmland Cadastral Data in Areas Subject to Landslides.” *ISPRS International Journal of Geo-Information* 7(8):331. doi: 10.3390/ijgi7080331.

QGIS Development Team. 2025. “QGIS Geographic Information System.”

R Core Team, R. 2025. “R: A Language and Environment for Statistical Computing.” *Foundation for Statistical Computing Vienna, Austria*.

Siriba, D. N., S. Dalyot, and M. Sester. 2012. “Geometric Quality Enhancement of Legacy Graphical Cadastral Datasets through Thin Plate Splines Transformation.” *Survey Review* 44(325):91–101. doi: 10.1179/1752270611Y.0000000011.

Sisman, Yasemin. 2014. “Coordinate Transformation of Cadastral Maps Using Different Adjustment Methods.” *Journal of the Chinese Institute of Engineers* 37(7):869–82. doi: 10.1080/02533839.2014.888800.

Tamim, Najeh Sadiq. 1992. “A Methodology to Create a Digital Cadastral Overlay through Upgrading Digitized Cadastral Data.” The Ohio State University, Ohio, USA.

Tong, Xiaohua, Wenzhong Shi, and Dajie Liu. 2009. “Introducing Scale Parameters for Adjusting Area Objects in GIS Based on Least Squares and Variance Component Estimation.” *International Journal of Geographical Information Science* 23(11):1413–32. doi: 10.1080/13658810802077826.

Tsolakis, Panos. 1996. *Urban Planning and Architectural Surveys in Kastoria;* Thessaloniki, Greece: University Studio Press.

Tuno, Nedim, Admir Mulahusić, and Dušan Kogoj. 2017. “Improving the Positional Accuracy of Digital Cadastral Maps through Optimal Geometric Transformation.” *Journal of Surveying Engineering* 143(3):05017002. doi: 10.1061/(ASCE)SU.1943-5428.0000217.

Valavi, Roozbeh, Jane Elith, José J. Lahoz-Monfort, and Gurutzeta Guillera-Arroita. 2019. “blockCV: An r Package for Generating Spatially or Environmentally Separated Folds for k-Fold Cross-Validation of Species Distribution Models.” *Methods in Ecology and Evolution* 10(2):225–32. doi: 10.1111/2041-210X.13107.

Veis, George. 1995. *Reference systems and the realization of the Helleni Geodetic Reference System 1987*. Athens, Greece: Technical Chamber of Greece.

Vorel, Branka, Bojan Barisic, Sinisa Hofer, and Ankica Hazdovac. 2010. “Cadastral Plan Geometric Accuracy Improvement.” P. 845 in *International Multidisciplinary Scientific GeoConference : SGEM*. Vol. 1. Sofia, Bulgaria: Surveying Geology & Mining Ecology Management (SGEM).

Watson, G. A. 2006. “Computing Helmert Transformations.” *Journal of Computational and Applied Mathematics* 197(2):387–94. doi: 10.1016/j.cam.2005.06.047.

Wierzbicki, Damian, Olga Matuk, and Elzbieta Bielecka. 2021. “Polish Cadastre Modernization with Remotely Extracted Buildings from High-Resolution Aerial Orthoimagery and Airborne LiDAR.” *Remote Sensing* 13(4):611. doi: 10.3390/rs13040611.

Wood, S. N. 2017. *Generalized Additive Models: An Introduction with R*. 2nd ed. NY, USA: Chapman and Hall/CRC.

Wood, Simon N. 2003. "Thin Plate Regression Splines." *Journal of the Royal Statistical Society Series B: Statistical Methodology* 65(1):95–114. doi: 10.1111/1467-9868.00374.

Wood, Simon N. 2010. "Fast Stable Restricted Maximum Likelihood and Marginal Likelihood Estimation of Semiparametric Generalized Linear Models." *Journal of the Royal Statistical Society Series B: Statistical Methodology* 73(1):3–36. doi: 10.1111/j.1467-9868.2010.00749.x.

Wood, Simon N., Natalya Pya, and Benjamin Säfken. 2016. "Smoothing Parameter and Model Selection for General Smooth Models." *Journal of the American Statistical Association* 111(516):1548–63. doi: 10.1080/01621459.2016.1180986.

Xu, K., M. Zhang, J. Li, S. Du, K. Kawarabayashi, and S. Jegelka. 2021. "How Neural Networks Extrapolate: From Feedforward to Graph Neural Networks." in *International Conference on Learning Representations (ICLR)*. Virtual Only Conference.

Zhu, Min, Handi Zhang, Anran Jiao, George Em Karniadakis, and Lu Lu. 2023. "Reliable Extrapolation of Deep Neural Operators Informed by Physics or Sparse Observations." *Computer Methods in Applied Mechanics and Engineering* 412:116064. doi: 10.1016/j.cma.2023.116064.

Zrinjski, Mladen, Đuro Barković, Antonio Tupek, and Ena Smoković. 2019. "Homogenization of the Cadastral Map of Cadastral Municipality Plomin in Croatia." Pp. 995–1004 in *7th International Conference Contemporary Achievements in Civil Engineering*. Subotica, Servia.